ACKNOWLEDGMENT

The authors wish to thank M. J. Marcoux of Giers, Schlumberger for his encouragement.

REFERENCES

[1] J Brian Davies, "A least-squares boundary residual method the numerical solution of scattering problems," *IEEE Trans. Microwave Theory Tech.*, vol. MTT-21, pp. 99–104, Feb. 1973.
[2] H. Lariviere and J. B. Davies, "The solution of electromagnetic eigenvalue problems by least-squares boundary residuals," *IEEE Trans. Microwave Theory Tech.*, vol. MTT-25, pp. 436–441, May 1975.
[3] J. Atechian, H. Baudrand, and J. Pahn, "Composite dielectric waveguide," *Electron. Lett.*, vol. 20, no. 4, pp. 189–190, Feb. 1984.
[4] H. Baudrand, T. El Khoury, and D. Lilonga, "Amplification by interdigital excitation of space-charge waves in semiconductors," *IEEE Trans Microwave Theory Tech.*, vol. MTT-32, pp. 1434–1441, Nov. 1984.
[5] J. Brian Davies, "Surface-acoustic wave propagation on a piezoelectric substrate with a periodic metal grating," *Electron. Lett.*, vol. 20, no. 18, pp. 720–722, Aug. 1984.
[6] R. Mittra and T. Itoh, "A new technique for the analysis of dispersion characteristics of microstrip lines," *IEEE Trans. Microwave Theory Tech.*, vol. MTT-19, pp. 47–56, Jan. 1971.
[7] R. Jansen, "A modified least-squares boundary residual method and its applications to the problem of shielded microstrip dispersion," *Arch. Elek. Übertragung.*, Band 28, Heft 6, pp. 275–277, 1974.
[8] K. C. Gupta, R. Garg, and I. J. Bahl, *Microstrip Lines and Slotlines*. Dedham, MA: Artech House, ch. 8, 1978.
[9] H. A. Wheeler, "Transmission line properties of parallel strips separated by a dielectric sheet," *IEEE Trans. Microwave Theory Tech.*, vol. MTT-13, pp. 172–185, Mar. 1965.
[10] T. Itoh and R. Mittra, "Spectral domain approach for calculating the dispersion characteristics of microstrip lines," *IEEE Trans. Microwave Theory Tech.*, vol. MTT-21, 1973.

Application of the Boundary-Element Method to Waveguide Discontinuities

MASANORI KOSHIBA, SENIOR MEMBER, IEEE, AND
MICHIO SUZUKI, SENIOR MEMBER, IEEE

Abstract—**A numerical method for the solution of scattering of the *H*- and *E*-plane waveguide junctions is described. The approach is a combination of the boundary-element method and the analytical method. A general computer program has been developed using the quadratic elements (higher order boundary elements). To show the validity and usefulness of this formulation, computed results are given for a right-angle corner bend, a T-junction, an inductive strip-planar circuit mounted in a waveguide, a waveguide-type dielectric filter, and an inhomogeneous waveguide junction, and a linear taper. Comparison of the present results with the results of the finite-element method shows good agreement.**

I. INTRODUCTION

Waveguide discontinuities play an important role in designing microwave circuits [1], [2], and theoretical and experimental studies of waveguide discontinuity scattering problems have occupied the attention of numerous researchers for several decades. Recently, a numerical approach based on the finite-element method (FEM) has been developed for the analysis of planar circuits [3], [4], and *H*- and *E*-plane waveguide junctions [5]–[7]. The FEM is very useful for the arbitrarily shaped discontinuities. However, it requires a large computer memory and long computation time to solve the final matrix equation. More recently, the boundary-element method (BEM) [8], [9] has been applied to the *H*-plane junctions [10]–[12] and the planar circuits [13]. The BEM is one of the 'boundary'-type methods based on the integral equation method which has already been successfully applied to open-boundary planar circuits in 1972 [14] and to short-boundary planar circuits in 1975 [15], [16]. It is therefore possible to reduce the matrix dimension and to use computer memory more economically compared with the 'domain'-type method, such as the FEM. However, in [10], [11], [14], and [15], it is assumed that the waveguide propagates a single mode only and the evanescent modes are neglected. Therefore, it seems to be difficult to obtain accurate results over a wide range of frequencies. Furthermore, in [10]–[16], the constant elements [8], [9] or the linear elements [8], [9] are used to divide the boundary of the two-dimensional region. Generally, it is difficult to reduce the energy error with these boundary elements. In [12], the linear elements are used and the condition of power conservation is satisfied to an accuracy of about ± 4 percent. In order to obtain more accurate results, fairly many elements are necessary, and, thus, the merits of the BEM are lost. In the FEM analysis using the quadratic triangular elements (higher order finite elements), on the other hand, the energy error is less than 0.1 percent [5]–[7].

In this paper, the combined method of the BEM with the quadratic line elements (higher order boundary elements) and the analytical method is described for the analysis of scattering by the *H*- or *E*-plane waveguide junctions. To show the validity and usefulness of this formulation, computed results are given for various *H*- and *E*-plane waveguide discontinuities. Comparison of the results of the BEM with those of the FEM [5]–[7] shows good agreement. In the present BEM analysis, the power condition is satisfied to an accuracy of $\pm 10^{-4}$ to 10^{-3}.

II. BASIC EQUATIONS

In order to minimize the detail, we consider the waveguide junction as shown in Fig. 1, where the boundary Γ_i connects the discontinuities to the rectangular waveguide i ($i=1, 2$), d_i is the width a_i or the height b_i of the waveguide i for the *H*- or *E*-plane junction, respectively; the region Ω surrounded by Γ_1, Γ_2, and the short-circuit boundary Γ_0 completely encloses the waveguide discontinuities, and the waveguide i is assumed to be filled with dielectric of relative permittivity ϵ_{ri}.

Considering the excitation by the dominant TE_{10} mode, we have the following basic equation:

$$\frac{\partial^2 \phi}{\partial x^2} + \frac{\partial^2 \phi}{\partial y^2} + \hat{k}^2 \phi = 0 \tag{1}$$

$$\hat{k}^2 = k_0^2 \hat{\epsilon}_r \tag{2}$$

$$k_0^2 = \omega^2 \epsilon_0 \mu_0 \tag{3}$$

$$\phi = \begin{cases} E_z, & \text{for } H\text{-plane junction} \\ H_z, & \text{for } E\text{-plane junction} \end{cases} \tag{4}$$

$$\hat{\epsilon}_r = \begin{cases} \epsilon_r, & \text{for } H\text{-plane junction} \\ \epsilon_r - (\pi/k_0 a)^2, & \text{for } E\text{-plane junction} \end{cases} \tag{5}$$

where ω is the angular frequency, E_z and H_z are the electric and

Manuscript received May 14, 1985; September 27, 1985.
The authors are with the Department of Electronic Engineering, Hokkaido University, Sapporo, 060, Japan.
IEEE Log Number 8406478.

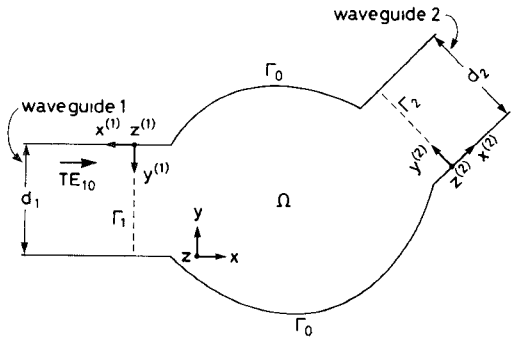

Fig. 1. Geometry of problem

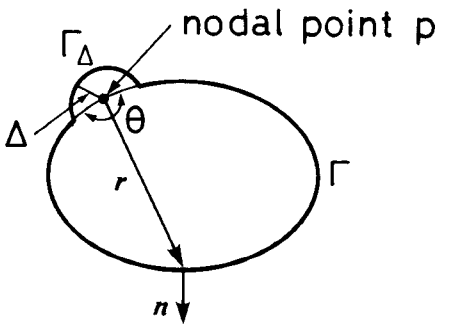

Fig 2. Two-dimensional region surrounded by boundary Γ.

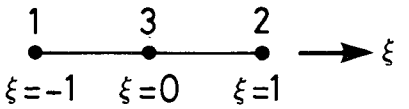

Fig 3. Quadratic line element.

magnetic fields, respectively, and ϵ_0 and μ_0 are the permittivity and permeability of free space, respectively.

III. Mathematical Formulation

A. Boundary-Element Approach[1]

Considering the region surrounded by the boundary Γ as shown in Fig. 2, and using the fundamental solution ϕ^* [8], [9] and Green's formula, from (1) we obtain the following equation [10]–[13]:

$$\phi_p + \int_\Gamma \psi^* \phi \, d\Gamma = \int_\Gamma \phi^* \psi \, d\Gamma \tag{6}$$

where

$$\phi^* = \frac{1}{4j} H_0^{(2)}(\hat{k}r) \tag{7}$$

$$\psi^* = \frac{j}{4} \hat{k} H_1^{(2)}(\hat{k}r) \cos\alpha. \tag{8}$$

Here ϕ_p is the value of ϕ at the nodal point p, ψ, and ψ^* are the outward normal derivatives of ϕ and ϕ^*, respectively, $H_0^{(2)}$ and $H_1^{(2)}$ are the zeroth- and first-order Hankel functions of the second kind, respectively, and α is the angle between the vector $\boldsymbol{r}$ and the outward unit normal vector $\boldsymbol{n}$.

Noting that the nodal point p is placed on the boundary Γ and considering the integration path Γ_Δ going around the nodal point p as shown in Fig. 2, we obtain for (6)

$$\frac{\theta}{2\pi}\phi_p + \oint_\Gamma \psi^* \phi \, d\Gamma = \oint_\Gamma \phi^* \psi \, d\Gamma \tag{9}$$

where $\oint$ denotes the Cauchy's principal value of integration, namely $\oint_\Gamma = \lim_{\Delta \to 0} \int_{\Gamma - \Gamma_\Delta}$. Dividing the boundary Γ into quadratic line elements as shown in Fig. 3, ϕ and ψ within each element are defined in terms of ϕ_q and ψ_q at the nodal points q ($q = 1, 2, 3$), respectively, as follows:

$$\phi = \{N\}^T \{\phi\}_e \tag{10}$$

$$\psi = \{N\}^T \{\psi\}_e \tag{11}$$

where

$$\{\phi\}_e = [\phi_1 \phi_2 \phi_3]^T \tag{12}$$

$$\{\psi\}_e = [\psi_1 \psi_2 \psi_3]^T \tag{13}$$

$$\{N\} = [N_1 N_2 N_3]^T. \tag{14}$$

[1]Since a general formulation of the BEM with linear elements for analyzing two-dimensional electromagnetic fields is given in [11], only the outline of the BEM with quadratic elements will be described here.

Here T, $\{\cdot\}$, and $\{\cdot\}^T$ denote a transpose, a column vector, and a row vector, respectively, and the shape function N_q is given by

$$N_q = A_q \xi^2 + B_q \xi + C_q \tag{15}$$

$$A_1 = 1/2, \quad A_2 = 1/2, \quad A_3 = -1 \tag{16a}$$

$$B_1 = -1/2, \quad B_2 = 1/2, \quad B_3 = 0 \tag{16b}$$

$$C_1 = 0, \quad C_2 = 0, \quad C_3 = 1 \tag{16c}$$

with the normalized coordinate ξ defined on the eth element.

Substituting (10) and (11) into (9), we obtain

$$\frac{\theta}{2\pi}\phi_p + \sum_e \{h\}_e^T \{\phi\}_e = \sum_e \{g\}_e^T \{\psi\}_e \tag{17}$$

where

$$\{h\}_e = [h_1 h_2 h_3]^T \tag{18}$$

$$\{g\}_e = [g_1 g_2 g_3]^T. \tag{19}$$

Here Σ_e extends over all different elements. When the nodal point p does not belong to the eth element, h_q and g_q are calculated with Gaussian integration as

$$h_q = \frac{L}{2} \int_{-1}^{1} N_q \frac{j}{4} \hat{k} H_1^{(2)}(\hat{k}r) \cos\alpha \, d\xi \tag{20}$$

$$g_q = \frac{L}{2} \int_{-1}^{1} N_q \frac{1}{4j} H_0^{(2)}(\hat{k}r) \, d\xi \tag{21}$$

where L is the length of the element. When the nodal point p belongs to the eth element, calculations of h_q and g_q involve the limitation of $\Delta \to 0$. In this case, $\cos\alpha = 0$, so that

$$h_q = 0. \tag{22}$$

For the case where the nodal point p coincides with the nodal point $q = 1$, 2, or 3 of the eth element in Fig. 2, g_q is given by

$$g_q = (L/2)\left[A_q I_2(2) - (2A_q - B_q)\{I_1(2) - 2/(\pi \hat{k}^2 L^2)\} + (A_q - B_q + C_q) I_0(2)\right] \tag{23a}$$

$$g_q = (L/2)\left[A_q I_2(2) - (2A_q + B_q)\{I_1(2) - 2/(\pi \hat{k}^2 L^2)\} + (A_q + B_q + C_q) I_0(2)\right] \tag{23b}$$

or

$$g_q = L\left[A_q I_2(1) + C_q I_0(1)\right] \tag{23c}$$

respectively. Here I_0, I_1, and I_2 are calculated as follows:

$$I_0(\eta) = \int \frac{1}{4j} H_0^{(2)}\left(\frac{\hat{k}L}{2}\eta\right) d\eta$$
$$= -\frac{\eta}{4} \sum_{v=0}^{\infty} \frac{(-1)^v}{(2v+1)(v!)^2} \left(\frac{\hat{k}L}{4}\eta\right)^{2v}$$
$$\cdot \left[\frac{2}{\pi}\left\{\gamma + \ln\left(\frac{\hat{k}L}{4}\eta\right) - \frac{1}{2v+1} - \sum_{s=1}^{v}\frac{1}{s}\right\} + j\right] \quad (24a)$$

$$I_1(\eta) = \int \frac{\eta}{4j} H_0^{(2)}\left(\frac{\hat{k}L}{2}\eta\right) d\eta$$
$$= \frac{1}{4j}\frac{2\eta}{\hat{k}L} H_1^{(2)}\left(\frac{\hat{k}L}{2}\eta\right) \quad (24b)$$

$$I_2(\eta) = \int \frac{\eta^2}{4j} H_0^{(2)}\left(\frac{\hat{k}L}{2}\eta\right) d\eta$$
$$= \left(\frac{2}{\hat{k}L}\right)^2 \left[\frac{\hat{k}L}{2}\frac{\eta^2}{4j} H_1^{(2)}\left(\frac{\hat{k}L}{2}\eta\right) + \frac{\eta}{4j} H_0^{(2)}\left(\frac{\hat{k}L}{2}\eta\right) - I_0(\eta)\right] \quad (24c)$$

where γ is the Euler's number.

In the matrix notation, (17) is rewritten as follows [8]–[13]:

$$[H]\{\phi\} = [G]\{\psi\}. \quad (25)$$

From (25), the following equation is obtained for the waveguide junction in Fig. 1:

$$[[H]_0 \quad [H]_1 \quad [H]_2]\begin{bmatrix}\{\phi\}_0\\ \{\phi\}_1\\ \{\phi\}_2\end{bmatrix} = [[G]_0 \quad [G]_1 \quad [G]_2]\begin{bmatrix}\{\psi\}_0\\ \{\psi\}_1\\ \{\psi\}_2\end{bmatrix} \quad (26)$$

where the subscripts 0, 1, and 2 denote the quantities corresponding to the boundaries Γ_0, Γ_1, and Γ_2 in Fig. 1, respectively.

B. Analytical Approach

Assuming that the dominant TE_{10} mode of unit amplitude is incident from the waveguide j ($j=1, 2$) in Fig. 1, ϕ on Γ_i ($i=1, 2$) may be expressed analytically as

$$\phi(x^{(i)}=0, y^{(i)}) = 2\delta_{ij} f_{j1}(y^{(j)}) - \sum_m \frac{1}{j\beta_{im}} \int_0^{d_i} f_{im}(y_0^{(i)}) f_{im}(y_0^{(i)}) \cdot \psi(x^{(i)}=0, y^{(i)})\, dy_0^{(i)} \quad (27)$$

where

$$f_{im}(y^{(i)}) = \sqrt{2/a_i}\sin m\pi y^{(i)}/a_i, \qquad m=1, 2, 3, \cdots \quad (28)$$

$$\beta_{im} = \sqrt{k_0^2\epsilon_{ri} - (m\pi/a_i)^2}, \qquad m=1, 2, 3, \cdots \quad (29)$$

for the H-plane junction

$$f_{im}(y^{(i)}) = \sqrt{\sigma_n/b_i}\cos n\pi y^{(i)}/b_i, \qquad n=0, 1, 2, \cdots \quad (30)$$

$$\beta_{im} = \sqrt{k_0^2\epsilon_{ri} - (\pi/a)^2 - (n\pi/b_i)^2}, \qquad n=0, 1, 2, \cdots \quad (31)$$

$$\sigma_n = \begin{cases}1, & n=0\\ 2, & n\neq 0\end{cases} \quad (32)$$

for the E-plane junction, and δ_{ij} is the Kronecker δ.

Using (10) and (11), (27) can be discretized as follows:

$$\{\phi\}_i = \delta_{ij}\{f\}_j + [Z]_i\{\psi\}_i \quad (33)$$

where

$$\{f\}_j = 2\{f_1\}_j \quad (34)$$

$$[Z]_i = -\sum_m (1/j\beta_{im})\{f_m\}_i \sum_{\dot{e}} \int_{\dot{e}} f_{im}(y_0^{(i)}) \cdot \{N(x^{(i)}=0, y_0^{(i)})\}\, dy_0^{(i)}. \quad (35)$$

Here the components of the $\{f_m\}_i$ vector are the values of $f_{im}(y^{(i)})$ at the nodal points on Γ_i and $\Sigma_{\dot{e}}$ extends over the elements related to Γ_i.

C. Combination of Boundary-Element and Analytical Relations

Using (33), from (26) we obtain the following final matrix equation:

$$\left[\begin{array}{cccccc} [H]_0 & [H]_1 & [H]_2 & -[G]_0 & -[G]_1 & -[G]_2 \\ \hline [0] & [1] & [0] & [0] & -[Z]_1 & [0] \\ [0] & [0] & [1] & [0] & [0] & -[Z]_2 \end{array}\right] \cdot \begin{bmatrix}\{\phi\}_0\\ \{\phi\}_1\\ \{\phi\}_2\\ \{\psi\}_0\\ \{\psi\}_1\\ \{\psi\}_2\end{bmatrix} = \begin{bmatrix}\{0\}\\ \{0\}\\ \{0\}\\ \{0\}\\ \hline \delta_{1j}\{f\}_j\\ \delta_{2j}\{f\}_j\end{bmatrix} \quad (36)$$

where [1] is a unit matrix, [0] is a null matrix, and $\{0\}$ is a null vector. In (36), $\{\phi\}_0 = \{0\}$ and $\{\psi\}_0 = \{0\}$ should be considered for the H- and E-plane junctions, respectively.

The values of ϕ at nodal points on Γ_i, namely $\{\phi\}_i$, are computed from (36), and then $\phi(x^{(i)}=0, y^{(i)})$ on Γ_i can be calculated from (10). The solutions on Γ_i allow the determination of the scattering parameters S_{ij} of the TE_{10} mode as follows:

$$S_{jj} = \int_0^{d_j} \phi(x^{(j)}=0, y^{(j)}) f_{j1}(y^{(j)})\, dy^{(j)} - 1 \quad (37)$$

$$S_{ij} = \sqrt{\beta_{i1}\hat{\epsilon}_{rj}/\beta_{j1}\hat{\epsilon}_{ri}} \cdot \int_0^{d_i} \phi(x^{(i)}=0, y^{(i)}) f_{i1}(y^{(i)})\, dy^{(i)}, \qquad i\neq j. \quad (38)$$

In (38), for the H-Plane junction, both $\hat{\epsilon}_{ri}$ and $\hat{\epsilon}_{rj}$ should be replaced by 1.

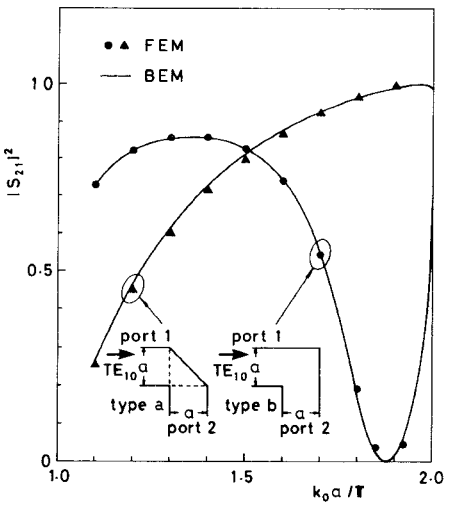

Fig. 4. Power transmission coefficient of right-angle corner bend.

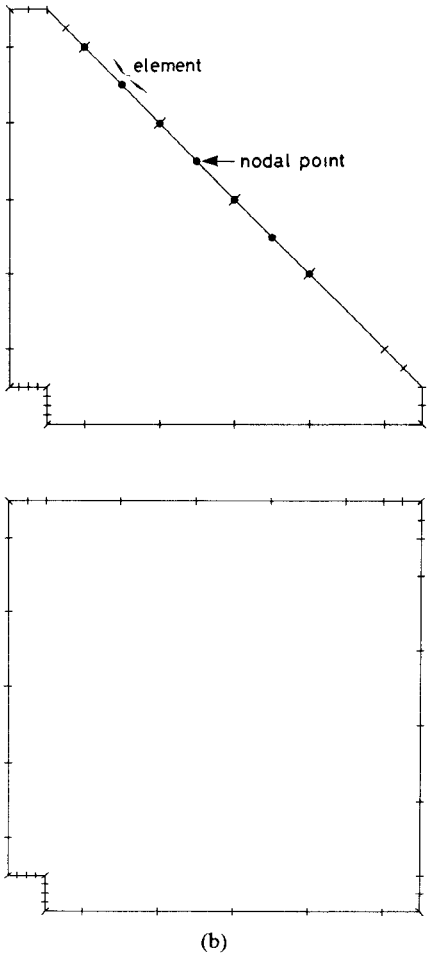

Fig. 5. Element division for right-angle corner bend

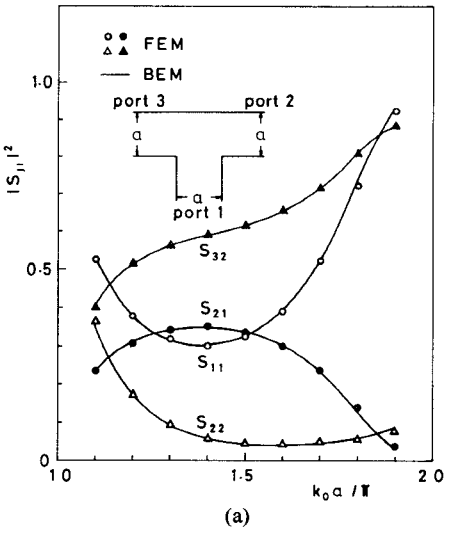

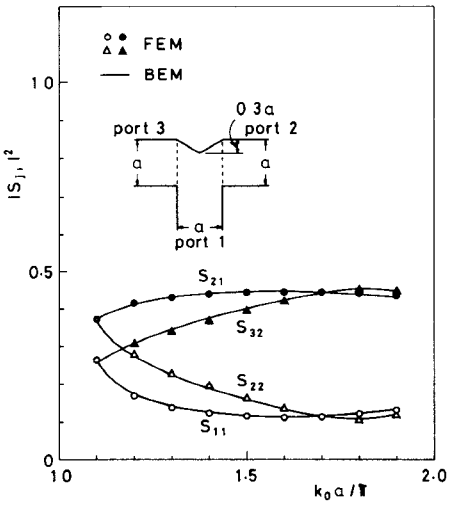

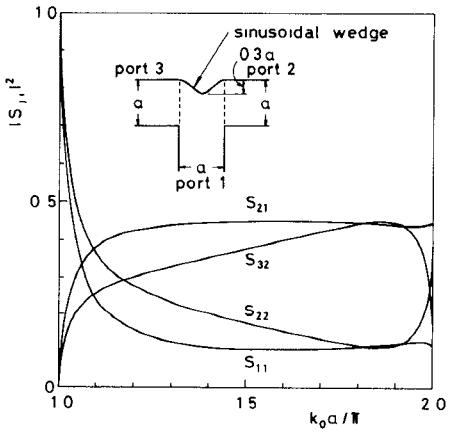

Fig. 6. Power reflection and transmission coefficients of T-junction.

IV. Computed Results

In this section, we present the computed results for various *H*- and *E*-plane waveguide discontinuities. Convergence of the solution is checked by increasing m in (35) and the number of the elements. Although the convergence is obtained by using the first three or four evanescent higher modes, in this analysis, the first six evanescent higher modes are used in (35). The results of the BEM agree well with those of the FEM [5]–[7] and agree well with the other theoretical results [15]–[20] and the experimental results [18], [19], [21]. For the *H*-plane waveguide discontinuities, the experimental results [18], [19] and the results of the integral equation method [15], [16], the normal-mode method [17]–[19], and the moment method [20] are not shown in this paper (these results are cited in [5] and [6]).

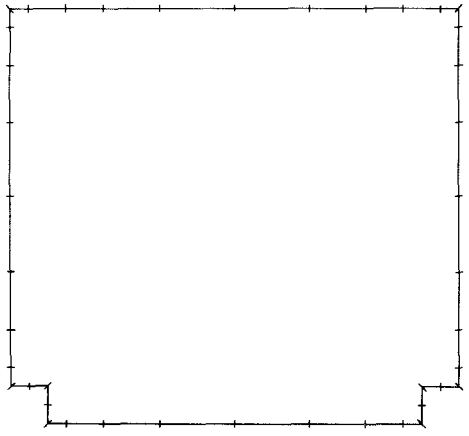

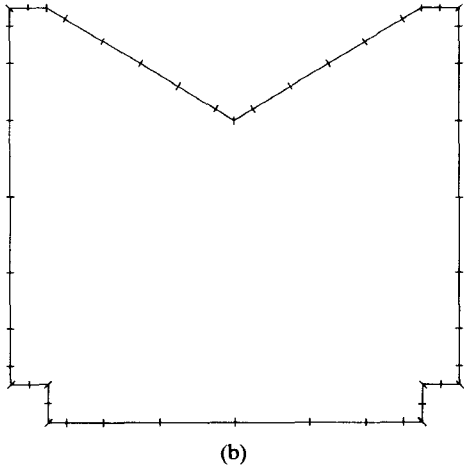

Fig. 7. Element division for T-junction

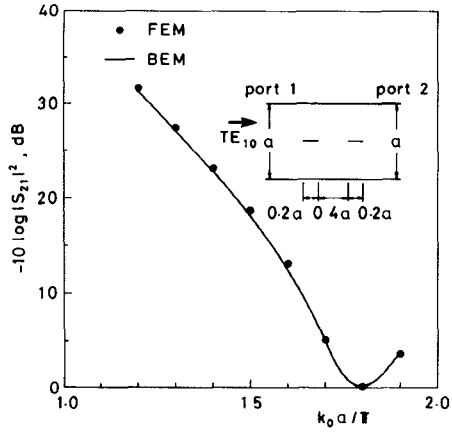

Fig. 8. Power transmission coefficient of inductive strip-planar circuit mounted in a waveguide.

A. H-Plane Junction

Fig. 4 shows the power transmission coefficient ($|S_{21}|^2$) of a right-angle corner bend. Fig. 5(a) and (b) shows the element divisions for the type *a* and the type *b* in Fig. 4, respectively.

The present approach can be applied easily to the analysis of multi-port junctions. Fig. 6 shows the power reflection coefficients ($|S_{11}|^2$ and $|S_{22}|^2$) and the power transmission coefficients ($|S_{21}|^2$ and $|S_{32}|^2$) of a T-junction. Fig. 7(a) and (b) shows the element divisions for the T-junction in Fig. 6(a) and the T-junction with wedge in Fig. 6(b), respectively. From Fig. 6(a)–(c), it is found that over a wide range of frequencies, the reflection at port 1 is reduced with a linear wedge (Fig. 6(b)) and that this reflection at port 1 may be further reduced with a sinusoidal wedge (Fig. 6(c)).

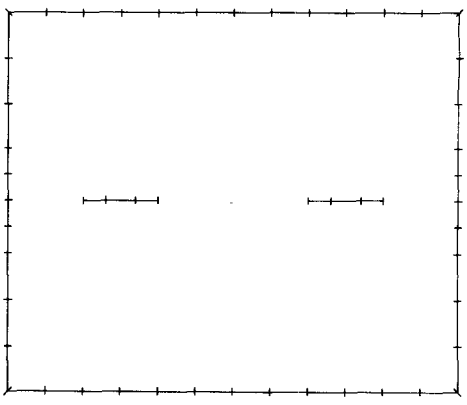

Fig. 9. Element division for inductive strip-planar circuit mounted in a waveguide.

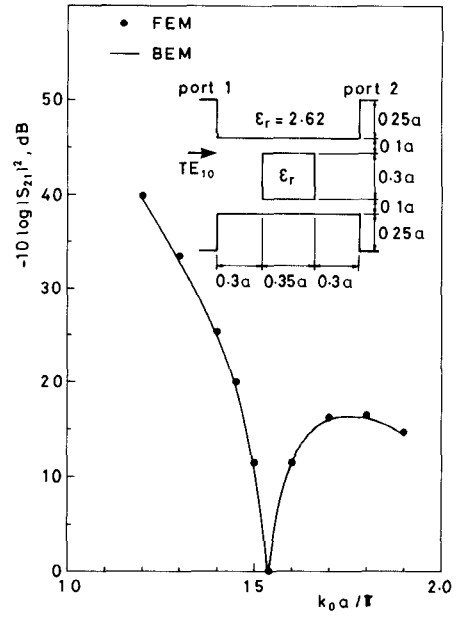

Fig. 10. Power transmission coefficient of waveguide-type dielectric filter.

Fig. 8 shows the power transmission coefficient of an inductive strip-planar circuit mounted in a waveguide. Fig. 9 shows the element division for this circuit. In this case, the boundary condition $\phi = 0$ should be considered on strip conductors.

The present approach can also be applied to the analysis of multi-media problems. A procedure of programming for handling multi-media problems is given in [11]. Fig. 10 shows the power transmission coefficient of a waveguide-type dielectric filter. Fig. 11 shows the element division for this filter. In this case, the boundary conditions $\phi_{air} = \phi_{dielectric}$ and $\psi_{air} = -\psi_{dielectric}$ should be considered on the interface between air and dielectric.

The present approach is applicable to the frequency range in which waveguide propagates multi-modes. Fig. 12(a) and (b) shows the magnitudes of reflection and transmission coefficients of an inhomogeneous waveguide junction, respectively. Fig. 13 shows the element division for this junction. For both reflection and transmission coefficients, the results of the BEM agree well with those of the FEM [6]. The results of the moment method [20] for the transmission coefficient are different from those of

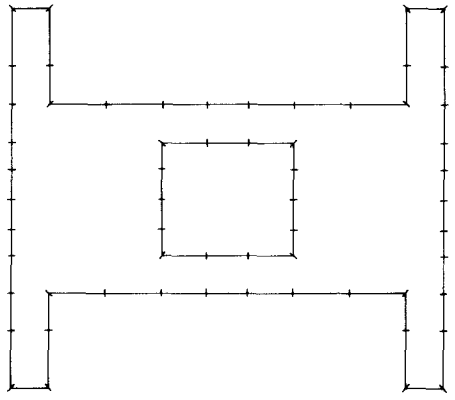

Fig. 11. Element division for waveguide-type dielectric filter.

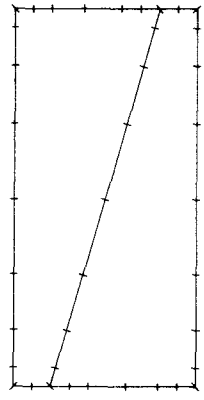

Fig 13. Element division for inhomogeneous waveguide junction.

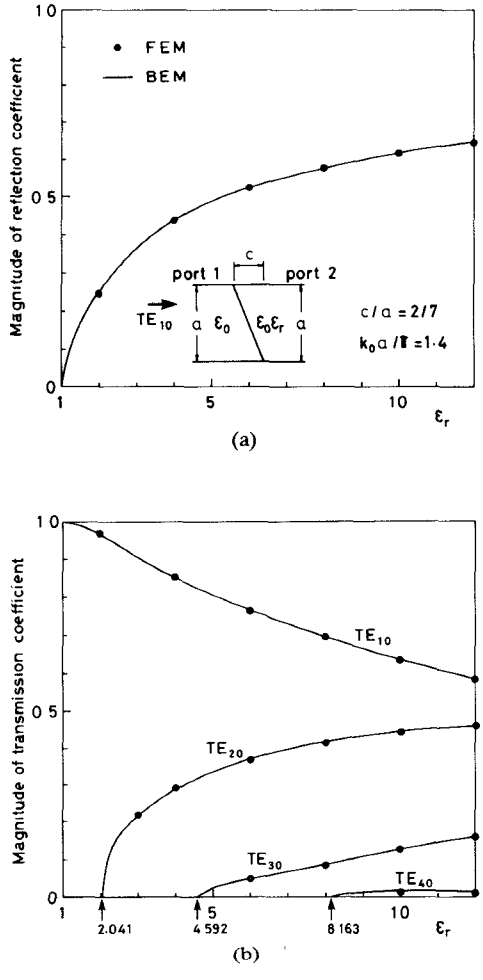

Fig. 12. Magnitudes of reflection and transmission coefficients of inhomogeneous waveguide junction

TABLE I
NUMBER OF NODAL POINTS USED IN THE BEM AND FEM ANALYSES

H-plane junction	BEM	FEM
Fig.4 (type a)	62	299
Fig.4 (type b)	76	377
Fig.6 (a)	84	385
Fig.6 (b)	96	399
Fig.8	102	609
Fig.10	120	379
Fig.12	79	589

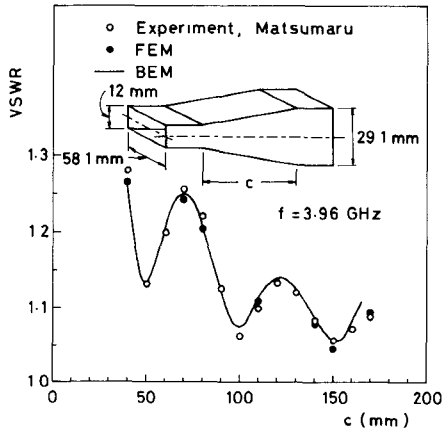

Fig. 14 VSWR characteristics of linear E-plane taper.

the BEM and the FEM. In the moment method, the transmission coefficients of the higher order modes are not zero at the cutoff values of ϵ_r.

Table I shows the number of the nodal points used in the BEM and FEM analyses of H-plane junctions. Here, in both BEM and FEM analyses, the symmetry of a circuit to reduce the dimensions of the matrices is not used. The accuracies of the present boundary-element calculations are almost identical to those of the earlier finite-element calculations [5], [6], and yet the BEM allows the matrix dimension to be reduced by a factor of about 7 to 3.

B. E-Plane Junction

A comparison of the results obtained applying the BEM to the linear E-plane tapers of various lengths with the experimental results [21] and the results of the FEM [7] is given in Fig. 14 and very good agreement is obtained.

V. CONCLUSION

A method of analysis, based on the boundary-element approach and the analytical approach, was developed for the solution of the H- and E-plane junctions. The validity of the method

was confirmed by comparing numerical results for various *H*- and *E*-plane waveguide discontinuities with the results of the finite-element method.

This approach can be applied easily to the planar circuits [3], [4], [13]. The problem of how to deal with waveguide junctions with lossy media or anisotropic media hereafter still remains.

ACKNOWLEDGMENT

The authors wish to thank T. Miki for his assistance in numerical computations.

REFERENCES

[1] N. Marcuvitz, *Waveguide Handbook*. New York: McGraw-Hill, 1951
[2] R. E. Collin, *Field Theory of Guided Waves*. New York: McGraw-Hill, 1960.
[3] P. Silvester, "Finite element analysis of planar microwave networks," *IEEE Trans. Microwave Theory Tech.*, vol. MTT-21, pp. 104–108, Feb. 1973.
[4] T. Miyoshi, "The expansion of electromagnetic field in planar circuit," *Trans. Inst. Electron. Commun. Eng. Japan*, vol. J58-B, pp. 84–91, Feb. 1975 (in Japanese).
[5] M. Koshiba, M. Sato, and M. Suzuki, "Application of finite-element method to *H*-plane waveguide discontinuities," *Electron. Lett.*, vol. 18, pp. 364–365, Apr. 1982.
[6] M. Koshiba, M. Sato, and M. Suzuki, "Finite-element analysis of arbitrarily shaped *H*-plane waveguide discontinuities," *Trans. Inst Electron Commun. Eng. Japan*, vol. E66, pp. 82–87, Feb. 1983.
[7] M. Koshiba, M. Sato, and M. Suzuki, "Application of finite-element method to *E*-plane waveguide discontinuities," *Trans. Inst. Electron. Commun. Eng. Japan*, vol. E66, pp. 457–458, July 1983.
[8] C. A. Brebbia, *The Boundary Element Method for Engineers*. London: Pentech Press, 1978.
[9] C. A. Brebbia and S. Walker, *Boundary Element Techniques in Engineering*. London: Butterworth, 1980.
[10] S. Washisu and I. Fukai, "An analysis of electromagnetic unbounded field problems by boundary element method," *Trans. Inst. Electron. Commun. Eng. Japan*, vol. J64-B, pp. 1359–1365, Dec. 1981 (in Japanese).
[11] S Kagami and I. Fukai, "Application of boundary-element method to electromagnetic field problems," *IEEE Trans. Microwave Theory Tech.*, vol. MTT-32, pp. 455–461, Apr. 1984.
[12] K. Kanao and S. Kurazono, "Waveguide-type dielectric filter," *Trans. Inst. Electron. Commun Eng. Japan*, vol. J67-B, pp. 1177–1178, Oct. 1984 (in Japanese).
[13] E. Tonye and H. Baudrand, "Multimode *S*-parameters of planar multiport junctions by boundary element method," *Electron. Lett.*, vol. 20, pp. 799–802, Sept. 1984.
[14] T. Okoshi and T. Miyoshi, "The planar circuit—An approach to microwave integrated circuitry," *IEEE Trans. Microwave Theory Tech.*, vol. MTT-20, pp. 245–252, Apr. 1972.
[15] T. Okoshi and S. Kitazawa, "Computer analysis of short-boundary planar circuit," *IEEE Trans. Microwave Theory Tech.*, vol. MTT-23, pp. 299–306, Mar. 1975.
[16] T. Okoshi and S. Kitazawa, "Computer analysis of short-boundary planar circuit," *Tech. Res. Rep. Inst. Electron. Commun. Eng. Japan*, MW75-75, Oct. 1975 (in Japanese).
[17] T. Anada and J. P. Hsu, "Analysis of planar circuit with short circuit boundary by normal mode method through impedance matrix," *Trans. Inst. Electron. Commun. Eng. Japan*, vol. J61-B, pp. 646–653, July 1978 (in Japanese).
[18] T. Anada, M. Hatayama, and J. P. Hsu, "Wide-band frequency characteristics of rectangular waveguide *H*-plane T-junctions," *Tech. Res. Rep. Inst. Electron. Commun. Eng. Japan*, MW79-68, Sept. 1979 (in Japanese).
[19] R. Monzen, N. Ogawa, T. Anada, and J P. Hsu, "Derivation of normal mode for dielectric planar circuit—Waveguide-type dielectric filter," *Tech. Res. Rep. Inst. Electron. Commun. Eng. Japan*, MW79-69, Sept. 1979 (in Japanese).
[20] Y. L. Chow and S. C. Wu, "A moment method with mixed basis functions for scattering by waveguide junctions," *IEEE Trans Microwave Theory Tech.*, vol. MTT-21, pp. 333–340, May 1973.
[21] K. Matsumaru, "Reflection coefficient of *E*-plane tapered waveguides," *IRE Trans. Microwave Theory Tech.*, vol. MTT-6, pp. 143–149, Apr. 1958.

A Frequency-Dependent Coupled-Mode Analysis of Multiconductor Microstrip Lines with Application to VLSI Interconnection Problems

EVERETT G. FARR, CHI H. CHAN, AND RAJ MITTRA, FELLOW, IEEE

***Abstract*—The spectral Galerkin procedure is used to calculate the dispersion properties of multiple conductor microstrip lines. The resulting propagation constants are then used in a coupled-mode theory which demonstrates a frequency-dependent coupling of current in a five-conductor system. These results should be useful in the study of crosstalk between parallel microstrip lines used in VLSI interconnections.**

I. INTRODUCTION

Recent advances in microelectronic packaging have generated certain difficulties associated with interconnections between VLSI logic devices. These interconnections are usually made with microstrip transmission lines, compactly etched on printed circuit boards. The performance of VLSI chips may be limited by the crosstalk between multiple parallel microstrip lines either within or between chips. Therefore, it is important to fully analyze multiple microstrip lines in order to determine the performance of the overall system. These crosstalk problems become more serious as switching speeds and packing densities are increased.

Coupled microstrip lines have been analyzed with several different methods in the past fifteen years [1]–[4]. More recently, multiconductor transmission lines have received some attention [5]–[9]. These analyses, however, are all based on a quasi-static approximation which is valid only for digital devices with switching speeds in the order of one nanosecond. When the rise-time of the switching pulse is reduced to tens of picoseconds, a full-wave analysis of multiconductor microstrip transmission lines becomes necessary.

The configuration under study is shown in Fig. 1. It is composed of five microstrip lines, each of the same width and strip separation. The object of this paper is to demonstrate, using a frequency-dependent analysis, the mechanism whereby current that is excited on one line is transferred to other lines. Although the VLSI interconnection problem is not addressed here directly, the technique presented herein could be employed for that purpose.

II. CALCULATION OF MODES

In order to analyze the crosstalk and propagation delay of the multiconductor transmission lines, the propagation constant for each of the propagating modes is needed. This may be calculated either with a quasi-static model, or with a frequency-dependent model. In this paper, the frequency-dependent model will be used, with the quasi-static model being used for comparison at lower frequencies.

Manuscript received June 13, 1985; revised September 30, 1985 This work was supported in part by the Office Naval Research under Grant N00014-85-K-0169 and in part by the Joint Services Electronics Program under Grant N00014-84-C-0149.

E. G Farr was with the Department of Electrical and Computer Engineering, University of Illinois. He is now with The BDM Corporation, 1801 Randolph Rd., S.E., Albuquerque, NM 87106

C. H Chan and R. Mittra are with the Department of Electrical and Computer Engineering, University of Illinois, 1406 W Green St., Urbana, IL 61801.

IEEE Log Number 8406479